

Probing the Permeability of Polyelectrolyte Multilayer Capsules via a Molecular Beacon Approach

Alexandra S. Angelatos, Angus P. R. Johnston, Yajun Wang, and Frank Caruso*

Centre for Nanoscience and Nanotechnology, Department of Chemical and Biomolecular Engineering,
The University of Melbourne, Parkville, Victoria 3010, Australia

Received December 20, 2006

Application of polyelectrolyte multilayer (PEM) capsules as vehicles for the controlled delivery of substances, such as drugs, genes, pesticides, cosmetics, and foodstuffs, requires a sound understanding of the permeability of the capsules. We report the results of a detailed investigation into probing capsule permeability via a molecular beacon (MB) approach. This method involves preparing MB-functionalized bimodal mesoporous silica (BMS_{MB}) particles, encapsulating the BMS_{MB} particles within the PEM film to be probed, and then incubating the encapsulated BMS_{MB} particles with DNA target sequences of different lengths. Permeation of the DNA targets through the capsule shell causes the immobilized MBs to open due to hybridization of the DNA targets with the complementary loop region of the MBs, resulting in an increase in the MB fluorescence. The assay conditions (BMS_{MB} particle concentration, MB loading within the BMS particles, DNA target concentration, DNA target size, pH, sodium chloride concentration) where the MB–DNA sensing process is effective were first examined. The permeability of DNA through poly(sodium 4-styrenesulfonate) (PSS)/poly(allylamine hydrochloride) (PAH) multilayer films, with and without a poly(ethyleneimine) (PEI) precursor layer, was then investigated. The permeation of the DNA targets decreases considerably as the thickness of the PEM film encapsulating the BMS_{MB} particles increases. Furthermore, the presence of a PEI precursor layer gives rise to less permeable PSS/PAH multilayers. The diffusion coefficients calculated for the DNA targets through the PEM capsules range from 10⁻¹⁹ to 10⁻¹⁸ m² s⁻¹. This investigation demonstrates that the MB approach to measuring permeability is an important new tool for the characterization of PEM capsules and is expected to be applicable for probing the permeability of other systems, such as membranes, liposomes, and emulsions.

Introduction

Polyelectrolyte multilayer (PEM) capsules are receiving interest as potential delivery vehicles in the areas of medicine, pharmaceuticals, and agriculture, and in the food and cosmetics industries.¹ However, to control both the loading of materials into such capsules and their subsequent release, a detailed understanding of capsule permeability is essential. PEM capsules are typically prepared by applying the layer-by-layer (LbL) assembly technique² to colloidal templates.³ This entails the (i) sequential deposition of polyelectrolytes (PEs) from solution onto nano- or microparticle cores, exploiting intermolecular forces such as electrostatic interactions or hydrogen bonding to drive the multilayer build-up, and (ii) decomposition of the templating particles to yield free-standing hollow capsules. The permeability of the capsules is influenced by the multilayer composition and thickness, as well as factors such as ionic strength, pH, temperature, solvent, and capsule age.¹

Several studies have investigated the permeability of PEM capsules. One method involves suspending preformed capsules in a probe solution and then using confocal laser scanning microscopy (CLSM) to monitor the permeation of the probe into individual capsules.⁴ A second, more quantitative method consists of encapsulating a crystalline material within the PEMs and then

adjusting the conditions to effect dissolution and hence release the core material into the bulk solution, which is subsequently extracted for analysis.^{5,6} Although these techniques require the diffusing species to be labeled with a fluorophore, they have yielded useful information regarding capsule permeability. There is, however, a need for a more efficient, sensitive, and accurate approach.

Recently, we introduced a molecular beacon (MB) technique to measure the permeability of PEM capsules (Scheme 1).⁷ A MB⁸ is a biosensor comprising a single-stranded (ss) DNA molecule with a fluorophore and a quencher at opposite ends. In its closed state, a MB forms a stem–loop structure, whereby the end regions of the DNA molecule (the stems) hybridize, bringing the fluorophore and quencher into close proximity such that the fluorescence is quenched. The central region of the DNA molecule remains ss, adopting a circular conformation (the loop). If a ssDNA sequence complementary to the loop (a DNA target) hybridizes with the loop, then the fluorophore and quencher separate such that the fluorescence is no longer quenched. In our

* To whom correspondence should be addressed. E-mail: fcaruso@unimelb.edu.au.

(1) (a) Johnston, A. P. R.; Cortez, C. M.; Angelatos, A. S.; Caruso, F. *Curr. Opin. Colloid Interface Sci.* **2006**, *11*, 203–209. (b) Peyratout, C. S.; Dähne, L. *Angew. Chem., Int. Ed.* **2004**, *43*, 3762–3783.

(2) (a) Decher, G.; Hong, J.-D. *Ber. Bunsen-Ges.* **1991**, *95*, 1430–1434. (b) Decher, G. *Science* **1997**, *277*, 1232–1237.

(3) (a) Caruso, F.; Caruso, R. A.; Möhwald, H. *Science* **1998**, *282*, 1111–1114. (b) Donath, E.; Sukhorukov, G. B.; Caruso, F.; Davis, S. A.; Möhwald, H. *Angew. Chem., Int. Ed.* **1998**, *37*, 2201–2205. (c) Caruso, F., Ed. *Colloids and Colloid Assemblies: Synthesis, Modification, Organization and Utilization of Colloidal Particles*; Wiley-VCH: Weinheim, 2003.

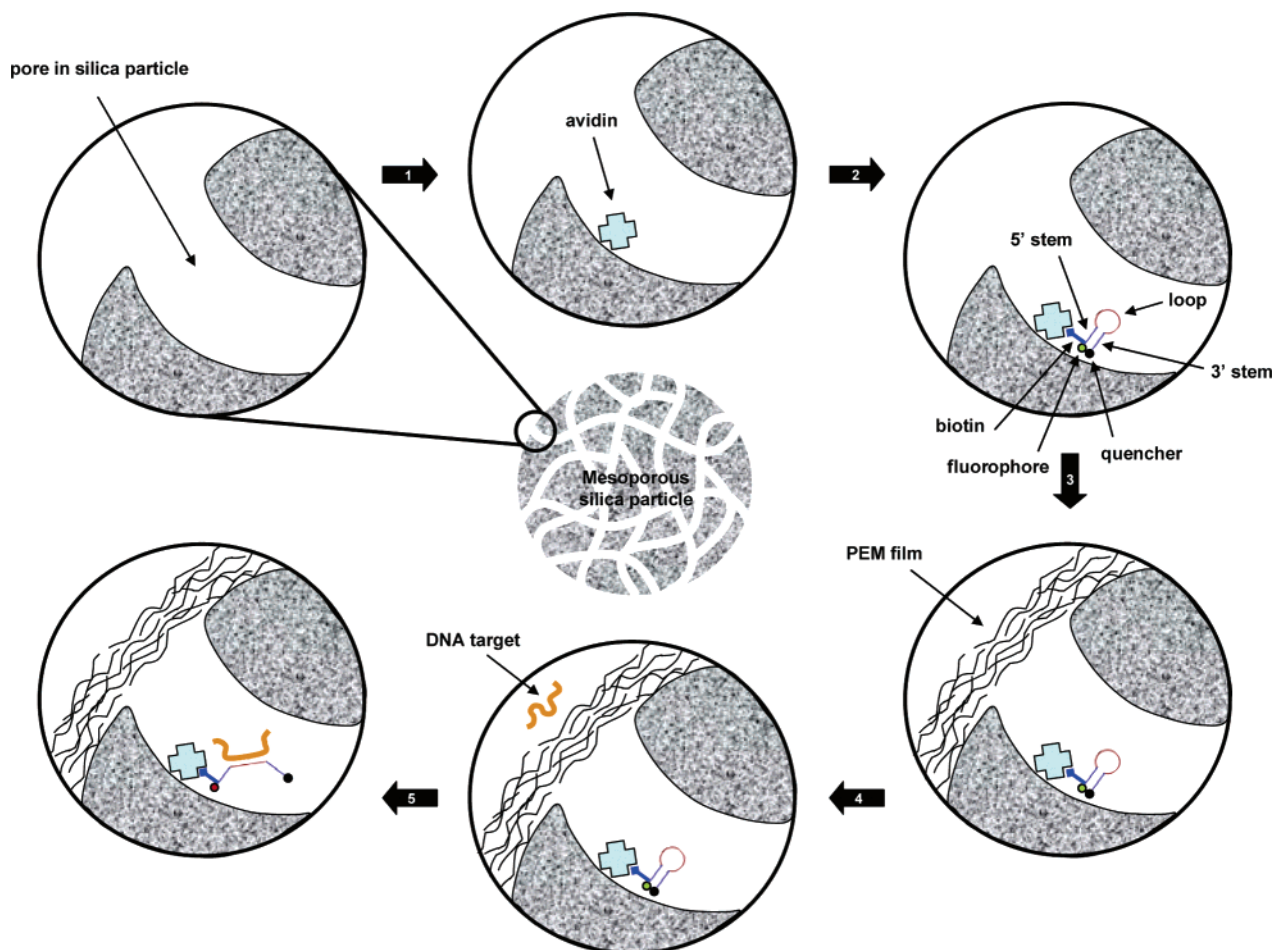
(4) (a) Ibarz, G.; Dähne, L.; Donath, E.; Möhwald, H. *Adv. Mater.* **2001**, *13*, 1324–1327. (b) Antipov, A. A.; Sukhorukov, G. B.; Leporatti, S.; Radtchenko, I. L.; Donath, E.; Möhwald, H. *Colloids Surf., A* **2002**, *198*, 535–541. (c) Berth, G.; Voigt, A.; Dautzenberg, H.; Donath, E.; Möhwald, H. *Biomacromolecules* **2002**, *3*, 579–590. (d) Georgieva, R.; Moya, S.; Hin, M.; Mitlöchner, R.; Donath, E.; Kiesewetter, H.; Möhwald, H.; Bäuml, H. *Biomacromolecules* **2002**, *3*, 517–524. (e) Ibarz, G.; Dähne, L.; Donath, E.; Möhwald, H. *Macromol. Rapid Commun.* **2002**, *23*, 474–478. (f) Ibarz, G.; Dähne, L.; Donath, E.; Möhwald, H. *Chem. Mater.* **2002**, *14*, 4059–4062.

(5) (a) Antipov, A. A.; Sukhorukov, G. B.; Donath, E.; Möhwald, H. *J. Phys. Chem. B* **2001**, *105*, 2281–2284. (b) Qiu, X. P.; Leporatti, S.; Donath, E.; Möhwald, H. *Langmuir* **2001**, *17*, 5375–5380. (c) Qiu, X. P.; Donath, E.; Möhwald, H. *Macromol. Mater. Eng.* **2001**, *286*, 591–597. (d) Antipov, A. A.; Sukhorukov, G. B.; Möhwald, H. *Langmuir* **2003**, *19*, 2444–2448. (e) Petrov, A. I.; Gavryushkin, A. V.; Sukhorukov, G. B. *J. Phys. Chem. B* **2003**, *107*, 868–875.

(6) Shi, X. Y.; Caruso, F. *Langmuir* **2001**, *17*, 2036–2042.

(7) Johnston, A. P. R.; Caruso, F. *J. Am. Chem. Soc.* **2005**, *127*, 10014–10015.

(8) Tyagi, S.; Kramer, F. R. *Nat. Biotechnol.* **1996**, *14*, 303–308.

Scheme 1. Schematic Illustration of the MB Approach to Measuring PEM Capsule Permeability^a

^a (1) Avidin is covalently attached inside the mesoporous silica particles. (2) Biotin-functionalized MBs are immobilized in the avidin-modified particles. (3) Particles are encapsulated within the PEM film to be probed. (4) Encapsulated particles are incubated with DNA targets. (5) DNA targets permeate through the capsule shell and open the MBs, and fluorescence is observed.

work, the MB approach to measuring the permeability of PEM capsules involves (i) immobilizing biotin-functionalized MBs inside bimodal mesoporous silica (BMS) particles⁹ that have been surface-modified with avidin (BMS_{MB}); (ii) applying the LbL assembly technique to coat the BMS_{MB} particles with the PEM films to be probed; and (iii) incubating the encapsulated BMS_{MB} particles with various DNA target sequences. During the incubation period, the increase in MB fluorescence, and hence the extent of DNA permeation through the capsule shell, may be monitored quantitatively via fluorescence spectroscopy and/or flow cytometry.⁷ The MB approach offers a number of advantages over existing methods employed to probe the permeability of PEM capsules. For example, it permits high throughput detection of extremely low concentrations of permeated DNA targets. Furthermore, the DNA targets do not require labeling and their size and conformation can be readily controlled by simply modifying their sequences. Importantly, the MB approach is expected to be widely applicable in that it could be used to study the permeability of other thin film-based systems (e.g., membranes, liposomes, emulsions). In addition, it could be used to study the permeation of other species besides DNA molecules, such as DNA conjugates, as DNA can be readily conjugated to various materials (e.g., nanoparticles, proteins).

Herein, we investigate the influence of parameters such as BMS_{MB} particle concentration, MB loading within the BMS

particles, DNA target concentration, DNA target size, pH, and sodium chloride (NaCl) concentration on the MB–DNA sensing process. We also report the use of the MB approach to probe the permeability of poly(sodium 4-styrenesulfonate) (PSS)/poly(allylamine hydrochloride) (PAH) multilayer films of different thicknesses, with and without a poly(ethyleneimine) (PEI) precursor layer. This work establishes the fundamental conditions required for MB sensing and paves the way for the widespread application of the MB approach in permeability studies.

Experimental Section

Materials. All materials were purchased from Sigma-Aldrich and used as received, except for the MB and the DNA target sequences, which were obtained from TriLink BioTechnologies (San Diego, CA) and GeneWorks (Adelaide, Australia), respectively. The average molecular weights of the PEs employed are 25 kDa (PEI), 70 kDa (PSS and PAH), and 86 kDa (fluorescein isothiocyanate (FITC)-labeled PSS). The water used was prepared in a three-stage Millipore Milli-Q Plus 185 purification system (resistivity, > 18.2 MΩ cm).

The sequences of the custom-synthesized MB and DNA targets are given in Table 1. The MB was designed with a 15 base (b) loop (bold) and 6 b stems (underlined), with the fluorophore Cyanine 3 (Cy3) coupled to the 5' end and Black Hole Quencher 2 (BHQ2) coupled to the 3' end. A biotin-modified thymidine residue was incorporated into the 5' stem to enable immobilization of the MB inside avidin-modified BMS particles. The bold text within each DNA target sequence corresponds to the region that is complementary to the MB loop.

(9) Wang, Y.; Yu, A.; Caruso, F. *Angew. Chem., Int. Ed.* **2005**, *44*, 2888–2892.

Table 1. Sequences of MB and DNA Targets

MB	5'-(Cy3)(biotin dT)GCTCGTCCATCTCATTCCAGCCGAGCA(BHQ2)-3'
15 b target	5'-GCTGAATGAGATGGA-3'
20 b target	5'-TACGCTGAATGAGATGGACG-3'
25 b target	5'-GCTACGCTGAATGAGATGGACGCAA-3'
30 b target	5'-ATGCTACGCTGAATGAGATGGACGCAAGCT-3'
35 b target	5'-GTAATGCTACGCTGAATGAGATGGACGCAAGCTCC-3'
60 b target	5'-GTGCCACAGGAAGTAATGCTACGCTGAATGAGATGGACGCAAGCTCCCCTCGCTGCTGGG-3'

Methods. Preparation of BMS_{MB} Particles. Avidin was covalently attached to the surface of 3-aminopropyltriethoxysilane (APTS)-modified BMS particles (particle diameter, 2–4 μm; pore diameters, 2–3 and 10–40 nm) as follows. First, 25 μL of an aqueous avidin solution (1 mg mL⁻¹) was added to 50 μL of an aqueous particle suspension (20 mg mL⁻¹). Then, 20 μL each of freshly prepared aqueous solutions of *N*-ethyl-*N'*-(3-dimethylaminopropyl)carbodiimide hydrochloride (100 mg mL⁻¹) and *N*-hydroxysuccinimide (20 mg mL⁻¹) were added to the particle suspension. The mixture was allowed to react at room temperature for 4 h with gentle agitation, after which the particles were washed via four cycles of centrifugation (1000g, 30 s), supernatant removal, and pellet redispersion in water. To confirm that the avidin was distributed homogeneously throughout the mesopores, 10 μL of the avidin-modified BMS particles were incubated with 10 μL of an aqueous FITC-biotin solution (1 mg mL⁻¹) for 10 min with continual mixing, after which the particles were washed via four cycles of centrifugation (1000g, 30 s), supernatant removal, and pellet redispersion in water. The biotin-functionalized MBs were immobilized inside the avidin-modified BMS particles (primarily inside the larger mesopores)⁹ by adding 1 μL of an aqueous MB solution (150 μM) to the avidin-modified BMS particle suspension for every milligram of BMS present (i.e., MB/BMS ratio of 1:1). The mixture was incubated for 10 min with continual mixing, after which the particles were washed via four cycles of centrifugation (1000g, 30 s), supernatant removal, and pellet redispersion in water.

Encapsulation of BMS_{MB} Particles. The BMS_{MB} particles were encapsulated within two different PEM films, namely, PSS/(PAH/PSS)_x and PEI/PSS/(PAH/PSS)_x, where *x* = 1, 2, 3, 4, or 6. The deposition of each PE layer involved incubating the particles in an aqueous polyelectrolyte (PE) solution (PE concentration, 1 mg mL⁻¹; NaCl concentration, 0.5 M) for 5 min with continual mixing, after which the particles were washed via four cycles of centrifugation (1000g, 30 s), supernatant removal, and pellet redispersion in water. This procedure was also used to coat BMS_{MB} particles with a single layer of FITC-PSS to confirm that, under the conditions employed in the LbL assembly (i.e., high PE molecular weight, low NaCl concentration, short adsorption time, no sonication during adsorption), the PEs primarily adsorb onto the outer particle surface rather than infiltrate the mesopores.⁹

Incubation with DNA Targets. The free MBs (i.e., MBs in solution) and the BMS_{MB} particles (with and without a PEM coating) were incubated with the DNA targets in sodium citrate buffer (citric acid concentration, 50 mM). The assay conditions used for each experiment are detailed in the figure captions.

The increase in MB fluorescence was monitored via fluorescence spectroscopy. Measurements were performed in 96-well plates (sample volume per well, 250 μL) using a HORIBA Jobin Yvon Fluorolog with a microwell plate reader (MicroMax 384): excitation wavelength, 550 nm; emission wavelength, 564 nm; integration time, 0.5 s. Typically, the MB (free or immobilized) solutions and the DNA target solutions were prepared at the desired assay conditions in Eppendorf tubes. The MB (free or immobilized) solutions (200 μL) were then added to the 96-well plate, followed by 50 μL of the DNA target solutions, and the solutions were mixed using a pipet.

Microscopy. The avidin-modified BMS particles loaded with FITC-biotin were imaged using an Olympus IX 71 inverted fluorescence microscope equipped with a FITC filter cube. The sample (1 μL) was placed onto a glass coverslip and viewed using a 60× oil immersion objective. The BMS_{MB} particles coated with a single layer of FITC-PSS were imaged using a Leica TCS SP2 AOBLS CLSM equipped with a picosecond pulsed diode laser

(excitation at 405 nm, fluorescence emission detected in the range 500–550 nm). The sample (1 μL) was placed onto a glass coverslip and viewed using a 63× oil immersion objective.

Results and Discussion

Investigation of the MB–DNA Sensing Process. Before encapsulating the BMS_{MB} particles within the PEM films to be probed, we investigated the influence of BMS_{MB} particle concentration, MB loading within the BMS particles, DNA target concentration, DNA target size, pH, and NaCl concentration on the MB–DNA sensing process.

First, the effect of BMS_{MB} particle concentration was examined to determine a suitable concentration of BMS_{MB} particles to conduct the assay. The MB fluorescence increases linearly with the BMS_{MB} particle concentration in the assay (see Supporting Information, Figure S1). This indicates that the MB fluorescence is not limited by the DNA target concentration over the BMS_{MB} particle concentration range investigated (2–16 × 10⁴ particles μL⁻¹), as the DNA target is in excess (see later). We did not consider higher concentrations of BMS_{MB} particles because the rate of increase in the MB fluorescence would decline as the DNA target becomes the limiting component. A BMS_{MB} particle concentration of 6 × 10⁴ particles μL⁻¹ was selected for the subsequent permeability experiments.

To investigate the influences of MB loading within the BMS particles and DNA target concentration on the MB–DNA sensing process, BMS_{MB} particles with different MB/BMS ratios (0.25:1, 0.5:1, and 1:1, which equate to ~2.25 × 10⁵, ~4.5 × 10⁵, and ~9 × 10⁵ MBs per particle, respectively) were prepared and incubated with a range of different DNA target concentrations (0.125–16 μM). Figure 1a shows the variation in MB fluorescence with DNA target concentration for various BMS_{MB} particles. Irrespective of the DNA target concentration in the assay, as the MB/BMS ratio increases, the MB fluorescence increases due to the higher loading of MBs within the BMS particles. Although the increase in MB fluorescence is not directly proportional to the increase in the MB/BMS ratio due to inter-MB quenching (see later), this result demonstrates that the sensitivity of the BMS_{MB} particles can be modified via the MB/BMS ratio. Similarly, irrespective of the MB/BMS ratio, the same trend is observed with respect to the MB fluorescence and DNA target concentration. Initially, as the concentration of the DNA target in the assay increases, there is a sharp increase in MB fluorescence, as the majority of the MBs are opened. Following this, the MB fluorescence increases only slightly or plateaus, as the remaining MBs are opened and the DNA target approaches excess levels. In the permeability experiments that follow, a MB/BMS ratio of 1:1 and a DNA target concentration of 3 μM were employed.

The effect of DNA target size (15–60 b) on MB fluorescence is shown in Figure 1b for free MBs in solution (plot A) and for MBs immobilized within BMS particles (plot B). For free MBs, the MB fluorescence increases with the length of the DNA target sequence, suggesting that the longer DNA targets are more efficient at opening the MBs. Importantly, the same trend is observed for immobilized MBs. This indicates that the BMS particle support has a negligible effect on the relative efficiency

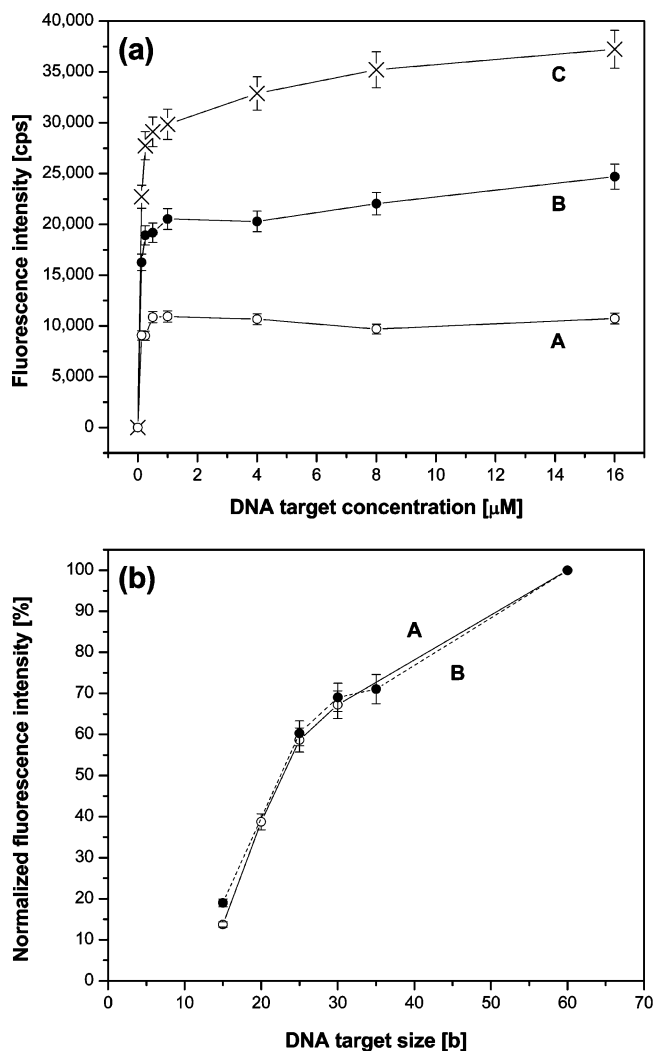


Figure 1. (a) Variation in MB fluorescence with DNA target concentration for BMS_{MB} particles prepared with a MB/BMS ratio of (A) 0.25:1, (B) 0.5:1, and (C) 1:1. Assay conditions: BMS_{MB} particle concentration, 8×10^4 particles μL^{-1} ; DNA target size, 30 b; pH, 7; NaCl concentration, 0.5 M; incubation time, 1 h. (b) Variation in normalized MB fluorescence with DNA target size for (A) free MBs and (B) immobilized MBs. Assay conditions (free MBs): MB concentration, $0.28 \mu\text{M}$; DNA target concentration, $0.4 \mu\text{M}$; pH, 7; NaCl concentration, 0.5 M; incubation time, 1 h. Assay conditions (immobilized MBs): BMS_{MB} particle concentration, 6×10^4 particles μL^{-1} ; MB/BMS ratio, 1:1; DNA target concentration, $3 \mu\text{M}$; pH, 7; NaCl concentration, 0.5 M; incubation time, 6 h.

with which the different DNA targets open the MBs. Immobilization of the MBs within BMS particles does, however, delay the MB–DNA sensing process since the DNA targets cannot access the MBs as quickly. For example, the maximum MB fluorescence produced by the 30 b target is achieved after 15 min for free MBs (Figure 2a, plot A) but after 6 h for immobilized MBs (Figure 2a, plot B). A possible explanation for why the longer DNA targets are more efficient at opening the MBs is because when the shortest DNA target (15 b) hybridizes with the 15 b MB loop, there is no DNA target “overhang” blocking the MB stems. Thus, the stem region of one open MB is free to hybridize with the complementary stem region of another open MB, resulting in inter-MB quenching (Scheme 2, part A). However, as the DNA target size increases, there is more DNA target “overhang”, and thus inter-MB quenching is increasingly unlikely for steric reasons (Scheme 2, part B). Inter-MB quenching

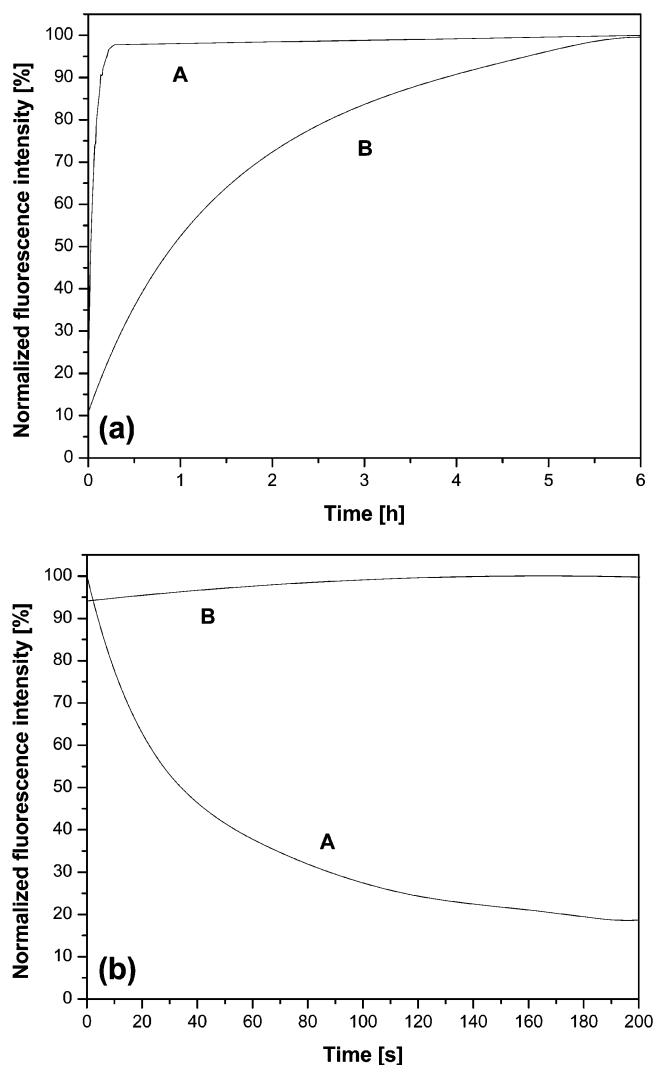
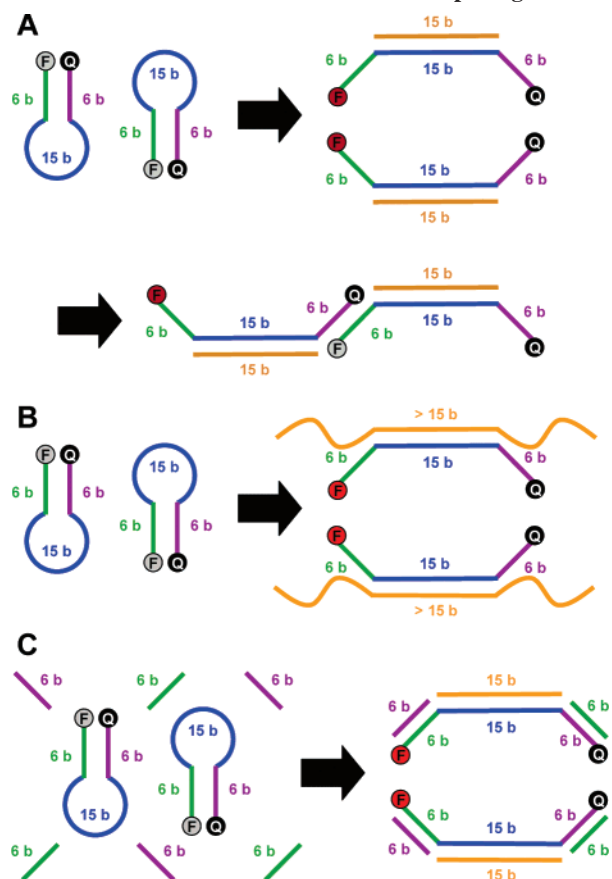


Figure 2. (a) Variation in normalized MB fluorescence with time for (A) free MBs and (B) immobilized MBs. Assay conditions (free MBs): MB concentration, $0.28 \mu\text{M}$; DNA target concentration, $0.4 \mu\text{M}$; DNA target size, 30 b; pH, 7; NaCl concentration, 0.5 M. Assay conditions (immobilized MBs): BMS_{MB} particle concentration, 5.6×10^4 particles μL^{-1} ; MB/BMS ratio, 1:1; DNA target concentration, $4 \mu\text{M}$; DNA target size, 30 b; pH, 7; NaCl concentration, 0.5 M. (b) Variation in normalized MB fluorescence with time for free MBs incubated in the (A) absence of the 6 b complementary sequences and (B) presence of a 10-fold excess of each 6 b complementary sequence (relative to the MB, i.e., $2.8 \mu\text{M}$). Assay conditions: MB concentration, $0.28 \mu\text{M}$; DNA target concentration, $0.4 \mu\text{M}$; DNA target size, 15 b; pH, 7; NaCl concentration, 0.5 M.

can be minimized by introducing an excess of 6 b DNA sequences that are complementary to the 6 b MB stem sequences (Scheme 2, part C). This was verified by incubating free MBs and the 15 b target together, with and without an excess of the 6 b complementary sequences. In the absence of the 6 b complementary sequences, the MB fluorescence decreases with time due to increasing inter-MB quenching (Figure 2b, plot A). In contrast, in the presence of an excess of the 6 b complementary sequences, the MB fluorescence increases with time because, although the 6 b complementary sequences themselves do not open the MBs (data not shown), they hybridize with the stem regions of the open MBs and thereby prevent inter-MB quenching (Figure 2b, plot B).

The permeability of a PEM film is sensitive to the pH and NaCl concentration of the adsorption solutions employed during

Scheme 2. Schematic Illustration of the Opening of MBs^a

^a (A) Opening of MBs by the 15 b target and the subsequent inter-MB quenching, (B) opening of MBs by DNA targets that are >15 b, and (C) opening of MBs by the 15 b target in the presence of an excess of 6 b DNA sequences that are complementary to the 6 b MB stem sequences.

LbL assembly, as well as the pH and NaCl concentration to which the film is exposed post-assembly.^{4a-d,5b-e} Before the MB approach can be used to probe the permeability of PEM capsules as a function of pH and NaCl concentration, it is important to examine the influence of these parameters on the MB–DNA sensing process. The MB fluorescence in the absence of DNA targets (i.e., the background fluorescence) is negligible, irrespective of the pH (2–11) and NaCl concentration (0–2 M) (data not shown). Thus, the MBs remain closed in the absence of DNA targets over the range of solution conditions examined. Also, the fluorophore Cy3 coupled to the 5' end of the MB is insensitive to pH (2–11) and NaCl concentration (0–2 M) (data not shown). Consequently, any variation in the MB fluorescence in the presence of DNA targets over the range of solution conditions examined may be attributed to differences in the MB–DNA interaction, rather than pH- or NaCl-induced changes in the fluorophore.

To examine the influence of pH, two distinct experiments were conducted. First, BMS_{MB} particles were exposed to a range of different pH values (2, 5, 7, 8, or 11) for 1 h prior to incubation of the particles with the DNA targets at pH 7. In a second experiment, BMS_{MB} particles were incubated with the DNA targets at a range of different pH values (2, 5, 7, 8, or 11). The NaCl concentration was fixed at 0.5 M in both experiments. Plot A in Figure 3a shows that while pretreatment with acidic pH has a minimal effect on the MB fluorescence, pretreatment with alkaline pH leads to a significant decrease in the MB fluorescence. As plot B in Figure 3a indicates, the trend observed when the

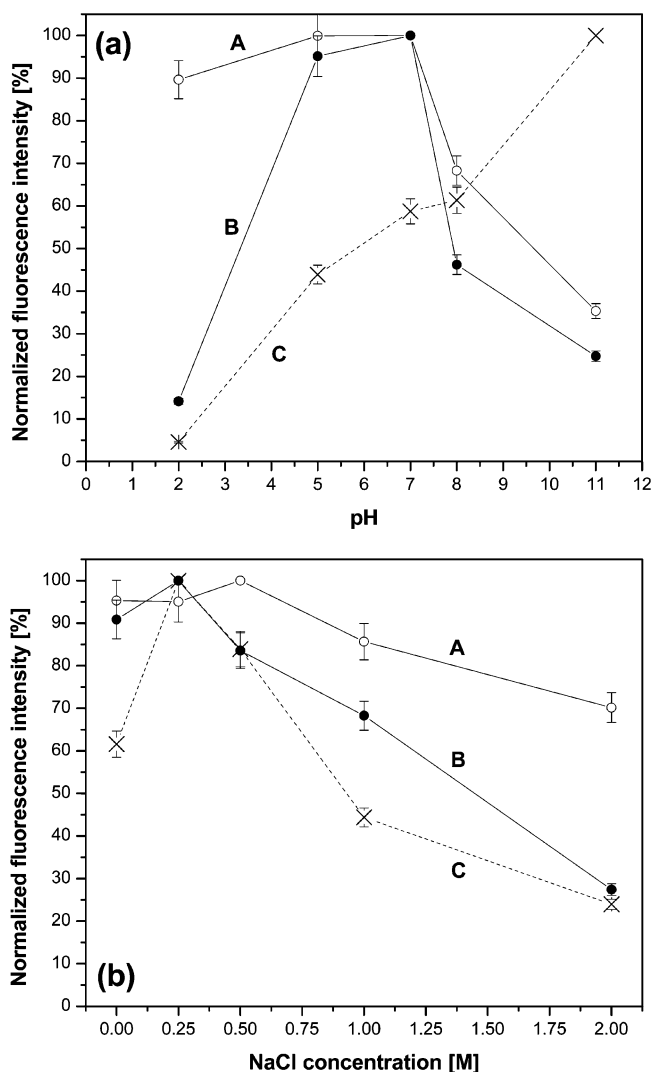


Figure 3. (a) Variation in normalized MB fluorescence with pH for (A) BMS_{MB} particles exposed to different pH values prior to incubation with the DNA targets at pH 7, (B) BMS_{MB} particles incubated with the DNA targets at different pH values, and (C) free MBs incubated with the DNA targets at different pH values. Assay conditions (immobilized MBs): BMS_{MB} particle concentration, 6×10^4 particles μL^{-1} ; MB/BMS ratio, 1:1; DNA target concentration, $3 \mu\text{M}$; DNA target size, 30 b; NaCl concentration, 0.5 M; incubation time, 1 h. Assay conditions (free MBs): MB concentration, $0.28 \mu\text{M}$; DNA target concentration, $0.4 \mu\text{M}$; DNA target size, 30 b; NaCl concentration, 0.5 M; incubation time, 1 h. (b) Variation in normalized MB fluorescence with NaCl concentration for (A) BMS_{MB} particles exposed to different NaCl concentrations prior to incubation with the DNA targets in 0.5 M NaCl, (B) BMS_{MB} particles incubated with the DNA targets in different NaCl concentrations, and (C) free MBs incubated with the DNA targets in different NaCl concentrations. Assay conditions (immobilized MBs): BMS_{MB} particle concentration, 6×10^4 particles μL^{-1} ; MB/BMS ratio, 1:1; DNA target concentration, $3 \mu\text{M}$; DNA target size, 30 b; pH, 7; incubation time, 1 h. Assay conditions (free MBs): MB concentration, $0.28 \mu\text{M}$; DNA target concentration, $0.4 \mu\text{M}$; DNA target size, 30 b; pH, 7; incubation time, 1 h.

pH during the assay is varied is similar to that observed when the pretreatment pH is varied, except that the MB fluorescence is greatly decreased at pH 2. These results suggest that alkaline pH induces a change in the BMS_{MB} particles, which has an adverse effect on the MB–DNA sensing process. This change appears to be irreversible since the MB fluorescence is considerably reduced not only when the particles are incubated with the DNA targets under alkaline conditions but also when the particles are

exposed to alkaline pH and then incubated with the DNA targets at pH 7 (i.e., the effect of pretreatment with alkaline pH is not fully reversed when the particles are returned to pH 7). These results also suggest that acidic pH has an adverse effect on the MB–DNA sensing process, since the MB fluorescence is considerably reduced when the particles are incubated with the DNA targets under acidic conditions. However, unlike alkaline pH, acidic pH does not induce an irreversible change in the BMS_{MB} particles, as the decrease in the MB fluorescence is negligible when the particles are exposed to acidic pH and then incubated with the DNA targets at pH 7.

To investigate these pH effects further, free MBs (i.e., MBs in solution) were incubated with the DNA targets at a range of different pH values (2, 5, 7, 8, or 11). It was found that the free MB fluorescence is considerably reduced when the assay is conducted at pH 2 (Figure 3a, plot C). This implies that the immobilized MB fluorescence is relatively low when the assay is conducted at pH 2 (Figure 3a, plot B) partly because the DNA targets do not hybridize as effectively with the MBs under extreme acidic conditions, possibly due to nucleotide protonation at low pH disrupting the complementary base pairing.¹⁰ In addition, it was found that the free MB fluorescence is unchanged when the assay is conducted at pH 8 and is considerably increased when the assay is conducted at pH 11 (Figure 3a, plot C). This indicates that the relatively low immobilized MB fluorescence obtained when the BMS_{MB} particles are pretreated with alkaline pH (Figure 3a, plot A) or when the assay is conducted at alkaline pH (Figure 3a, plot B) is due to a pH-induced change in the BMS_{MB} particles. Therefore, pH 7 was chosen as the optimum pH for conducting the assay in the subsequent permeability experiments.

The influence of NaCl concentration was examined in a similar manner to the pH study above. First, the BMS_{MB} particles were exposed to a range of different NaCl concentrations (0, 0.25, 0.5, 1, or 2 M) for 1 h prior to incubation of the particles with the DNA targets in 0.5 M NaCl. Then, the BMS_{MB} particles were incubated with the DNA targets in a range of different NaCl concentrations (0, 0.25, 0.5, 1, or 2 M). The pH was fixed at 7 in both experiments. As Figure 3b illustrates, the variation in the MB fluorescence is relatively minor when the BMS_{MB} particles are pretreated with NaCl concentrations below 0.5 M (Figure 3b, plot A) or when the assay is conducted in less than 0.5 M NaCl (Figure 3b, plot B). The MB fluorescence is, however, considerably reduced when the BMS_{MB} particles are pretreated with NaCl concentrations above 0.5 M (Figure 3b, plot A) or when the assay is conducted in greater than 0.5 M NaCl (Figure 3b, plot B). This suggests that high ionic strength induces an irreversible change in the BMS_{MB} particles (which has an adverse effect on the MB–DNA sensing process) since the effect of pretreatment with high NaCl concentrations is not fully reversed when the particles are returned to 0.5 M NaCl.

To investigate this NaCl effect further, free MBs (i.e., MBs in solution) were incubated with the DNA targets in a range of different NaCl concentrations (0, 0.25, 0.5, 1, or 2 M). It was found that the free MB fluorescence is significantly lower when the assay is conducted in the presence of high concentrations of NaCl (Figure 3b, plot C). These results suggest that high ionic strength (>0.05 M NaCl) not only adversely affects the BMS_{MB} particles (Figure 3b, plots A and B) but also hampers the hybridization between MBs and DNA targets, whether the MBs are free or immobilized, possibly because the DNA targets adopt a highly coiled conformation under such conditions. Thus, 0.5

M was selected as a suitable NaCl concentration for conducting the assay in the permeability experiments that follow.

Based on the above findings on the MB–DNA sensing process, the following conditions were chosen for the subsequent permeability experiments: BMS_{MB} particle concentration, 6×10^4 particles μL^{-1} ; MB/BMS ratio, 1:1; DNA target concentration, 3 μM ; pH, 7; NaCl concentration, 0.5 M.

Investigation of PEM Capsule Permeability. The LbL assembly technique was employed to encapsulate the BMS_{MB} particles within PEM films, the permeabilities of which were probed as a function of layer number, DNA target size, and incubation time. The various conditions used in the encapsulation process are detailed in the Experimental Section above.

Effect of Layer Number. We investigated the permeability of PSS/(PAH/PSS)_x films (where $x = 1, 2, 3, 4, \text{ or } 6$), with and without an initial layer of PEI (a PE used extensively as a precursor in LbL assembly on both planar and colloidal substrates). The outer layer was always PSS to avoid electrostatic interaction between the PEM films and the DNA targets. Quartz crystal microbalance (Q-Sense) measurements confirmed that the DNA targets do not bind to the PEM films with PSS as the outer layer (data not shown).

Figure 4a is a fluorescence microscopy image of avidin-modified BMS particles loaded with FITC-biotin. The fluorescence observed (originating from the FITC label on the biotin) is distributed homogeneously across the particle cross sections. This indicates that the biotin, and in turn avidin, are distributed homogeneously throughout the mesopores, and thus it is assumed that the biotin-functionalized MBs also infiltrate the avidin-modified BMS particles in a uniform manner. Figure 4b is a CLSM image of BMS_{MB} particles coated with a single layer of FITC-PSS under the same conditions used to construct the PEM films. In contrast to Figure 4a, the fluorescence observed (originating from the FITC label on the PSS) is concentrated at the outer surface of the particles. This indicates that, under the conditions employed in the LbL assembly, there is minimal infiltration of the PEs into the mesopores, and hence PEM films are formed on the outer surface of the particles.⁹ It is assumed that the PSS/PAH multilayer films formed on the outer surface of the BMS_{MB} particles are comparable in thickness to PSS/PAH multilayer films assembled on nonporous particles under similar conditions.¹¹ However, even if the PEM films formed on the BMS_{MB} particles and the nonporous particles differ in thickness by a factor of, for example, two, the permeabilities and diffusion coefficients reported below remain the same in terms of order of magnitude.

To estimate the permeability of the DNA targets through the PEM films, the following equation^{4e,f} was employed:

$$I(t) = I_0 + (I_s - I_0)(1 - e^{-3Pt/r}) \quad (1)$$

where $I(t)$ is the MB fluorescence intensity [cps] at time t [s], I_0 and I_s are the MB fluorescence intensities at $t = 0$ and $t \rightarrow \infty$, respectively, P is the DNA target permeability [m s^{-1}], and r is the capsule radius [m]. Equation 1 models our fluorescence data well, with a typical R^2 value of >0.99 (see Supporting Information, Figure S2). Mohwald and co-workers originally developed equation 1 to model the permeation kinetics of fluorescein through hollow PSS/PAH capsules.^{4e,f} Figure 5a illustrates the variation in the permeation of the 30 b target into the BMS_{MB} particles with the number of layers (PSS, PAH) encapsulating the particles. In the absence of a PEI precursor

(10) Puppels, G. J.; Otto, C.; Greve, J.; Robert-Nicoud, M.; Arndt-Jovin, D. J.; Jovin, T. M. *Biochemistry* **1994**, *33*, 3386–3395.

(11) Caruso, F.; Lichtenfeld, H.; Donath, E.; Mohwald, H. *Macromolecules* **1999**, *32*, 2317–2328.

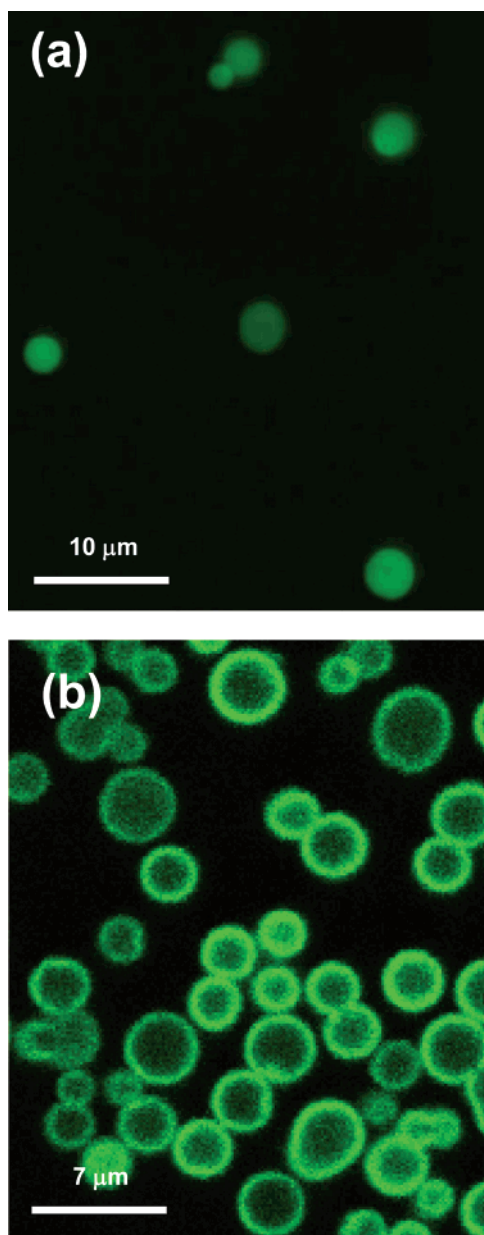


Figure 4. (a) Fluorescence microscopy image of avidin-modified BMS particles loaded with FITC-biotin. The homogeneous fluorescence observed arises from the FITC label on the biotin and indicates that the biotin, and hence avidin, are distributed homogeneously throughout the mesopores. (b) CLSM image of BMS_{MB} particles coated with a single layer of FITC-PSS. The ring fluorescence observed arises from the FITC label on the PSS and indicates that the polyanion is concentrated at the outer particle surface. Note that, for the BMS_{MB} particles, the biotin (incorporated into the 5' MB stem) is not labeled with FITC. See the Experimental Section above for details regarding the preparation of the particles imaged in parts a and b.

layer (Figure 5a, plot A), the permeability of the DNA target decreases from 2.1×10^{-10} to 2.8×10^{-11} m s⁻¹ as the layer number increases from 3 to 7, with negligible permeability being observed once the capsule shell comprises 9 layers. In the presence of a PEI precursor layer (Figure 5a, plot B), the permeability of the DNA target decreases from 1.5×10^{-10} to 2.5×10^{-11} m s⁻¹ as the layer number increases from 3 to 5, with negligible permeability being observed once the capsule shell comprises 7 layers. Importantly, the permeation of the 30 b target into the BMS_{MB} particles with no PSS/PAH multilayers is the same whether the particles are coated with a PEI precursor layer or

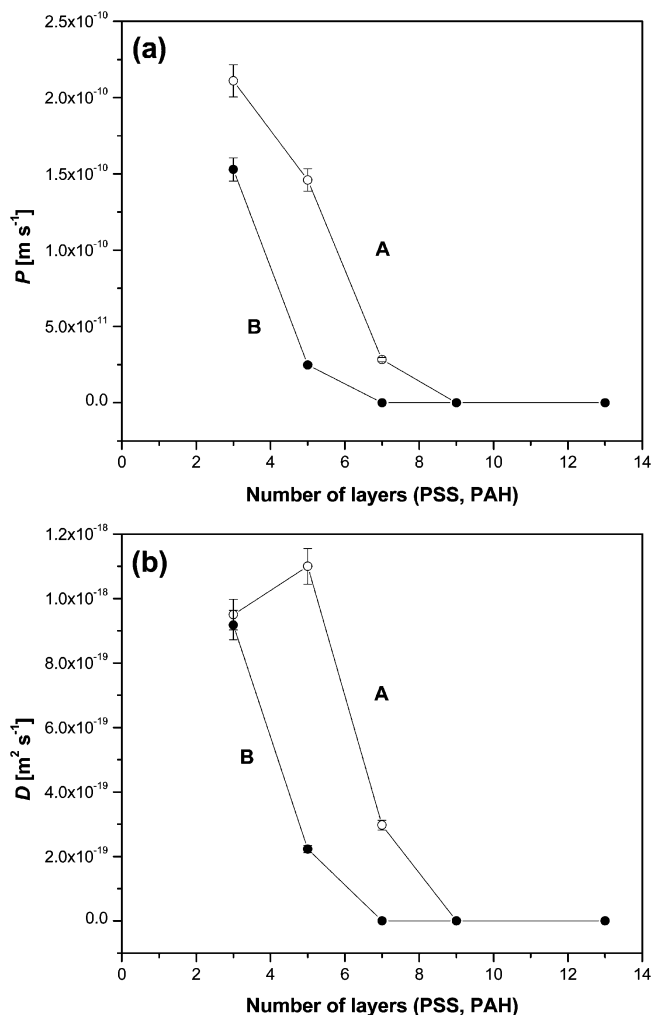


Figure 5. (a) Variation in P with layer number for (A) BMS_{MB} particles without a PEI precursor layer and (B) BMS_{MB} particles with a PEI precursor layer. Assay conditions: BMS_{MB} particle concentration, 6×10^4 particles μL^{-1} ; MB/BMS ratio, 1:1; DNA target concentration, 3 μM ; DNA target size, 30 b; pH, 7; NaCl concentration, 0.5 M. (b) Variation in D with layer number for (A) BMS_{MB} particles without a PEI precursor layer and (B) BMS_{MB} particles with a PEI precursor layer. Assay conditions are the same as those given in part a.

not. These results imply that, while the PEI precursor layer itself does not alter the permeability of the DNA target, its presence promotes the growth of less permeable PSS/PAH multilayers.

The diffusion coefficient of the DNA targets through the PEM films may be defined as^{4e,f}

$$D = Pd \quad (2)$$

where D is the DNA target diffusion coefficient [m² s⁻¹], P is the DNA target permeability [m s⁻¹], and d is the PEM film thickness [m]. Equation 2 assumes that the solubility coefficient of the DNA targets is unity (i.e., the DNA target concentration at the solution–film interface is the same as that in the bulk solution). We consider this simplifying assumption to be valid given that a large excess of the DNA targets was used in the assays. As the number of layers (PSS, PAH) encapsulating the BMS_{MB} particles increases, d increases and, as Figure 5a demonstrates, P decreases. The resulting variation in D with layer number is shown in Figure 5b. In the absence of a PEI precursor layer (Figure 5b, plot A), D decreases significantly following the deposition of 7 layers and is negligible once the capsule shell is 9 layers thick. In the presence of a PEI precursor

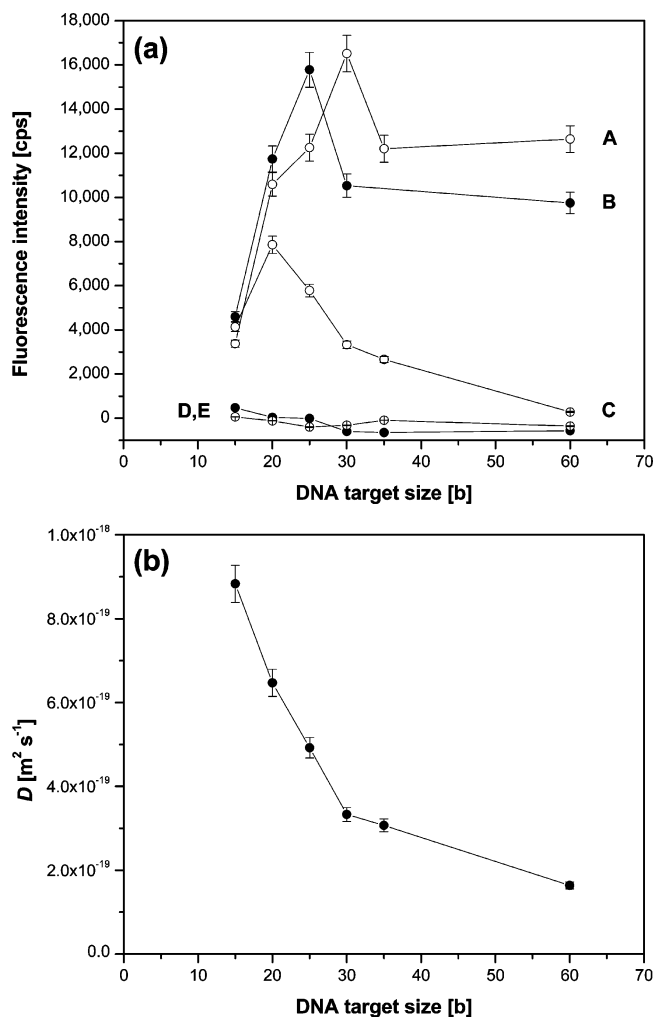


Figure 6. (a) Variation in MB fluorescence with DNA target size for BMS_{MB} particles encapsulated within (A) PSS/PAH/PSS (3 layers), (B) PSS/(PAH/PSS)₂ (5 layers), (C) PSS/(PAH/PSS)₃ (7 layers), (D) PSS/(PAH/PSS)₄ (9 layers), and (E) PSS/(PAH/PSS)₆ (13 layers). Assay conditions: BMS_{MB} particle concentration, 6×10^4 particles μL^{-1} ; MB/BMS ratio, 1:1; DNA target concentration, $3 \mu\text{M}$; pH, 7; NaCl concentration, 0.5 M; incubation time, 1 h. (b) Variation in D with DNA target size for BMS_{MB} particles encapsulated within PSS/(PAH/PSS)₃. Assay conditions: BMS_{MB} particle concentration, 6×10^4 particles μL^{-1} ; MB/BMS ratio, 1:1; DNA target concentration, $3 \mu\text{M}$; pH, 7; NaCl concentration, 0.5 M.

layer (Figure 5b, plot B), D decreases significantly following the deposition of 5 layers and is negligible once the capsule shell is 7 layers thick. Also, the fact that the variation in D (i.e., Pd) with layer number (Figure 5b) is similar to the variation in P with layer number (Figure 5a) indicates that, as the layer number increases, the trend in P clearly outweighs the opposing trend in d ; that is, the permeability dominates the diffusion coefficient.

Effect of DNA Target Size. Figure 6a shows the permeation of the different DNA targets as a function of the number of PE layers encapsulating the BMS_{MB} particles. For bare BMS_{MB} particles, the 60 b target gives rise to the highest MB fluorescence (Figure 1b, plot B). As the thickness of the PEM film encapsulating the BMS_{MB} particles increases, the size of the DNA target that produces the highest MB fluorescence decreases from 30 b (3 layers) to 25 b (5 layers) to 20 b (7 layers) to 15 b (9 or more layers) (Figure 6a). As was noted earlier, the fluorescence from bare BMS_{MB} particles is highest with the longest DNA target (60 b) since it is the most efficient at opening the MBs. However, for immobilized MBs in the presence of PEMs, the MB–DNA sensing process involves a balance between the efficiency with

which the DNA targets open the MBs and the efficiency with which the DNA targets diffuse toward the MBs. Just as the longer DNA targets are more efficient at opening the MBs, the shorter DNA targets are more efficient at permeating through the capsule shell to the MBs. Therefore, as the thickness of the capsule shell increases from 3 layers to 9 or more layers and DNA target permeation increasingly becomes the rate determining step in the MB–DNA sensing process, the size of the DNA target most efficient at both diffusing toward and opening the MBs decreases from 30 to 15 b. This progression demonstrates that PSS/PAH capsules can be readily tailored to preferentially include/exclude certain DNA sequences by simply tuning the capsule permeability through layer number. For example, consider the permeation of the different DNA targets into BMS_{MB} particles encapsulated within PSS/(PAH/PSS)₃ (Figure 6b). D decreases $\sim 63\%$ (from 8.8×10^{-19} to 3.3×10^{-19} $m^2 s^{-1}$) as the DNA target size doubles from 15 to 30 b. However, doubling the DNA target size again from 30 to 60 b leads to a further reduction in D of only $\sim 19\%$ (from 3.3×10^{-19} to 1.6×10^{-19} $m^2 s^{-1}$). This implies that 30 b is the critical DNA target size for 7-layer PSS/PAH capsules. That is, the PSS/(PAH/PSS)₃ shell is readily permeable to DNA targets < 30 b (the smaller the DNA target, the greater its permeability) but is relatively impermeable to DNA targets > 30 b (since minimal permeability is observed whether the DNA target is 30 or 60 b).

Effect of Incubation Time. The influence of incubation time on the permeation of the different DNA targets into BMS_{MB} particles encapsulated within PSS/(PAH/PSS)₃ is demonstrated in Figure 7. For bare BMS_{MB} particles, the maximum MB fluorescence is reached within hours of introducing the DNA targets (Figure 2a, plot B). In contrast, for encapsulated BMS_{MB} particles, the MB fluorescence increases gradually over days, with each DNA target size yielding a unique time curve (Figure 7a). Given that the DNA targets open the immobilized MBs more rapidly in the absence of a capsule shell, the MB–DNA sensing process for encapsulated BMS_{MB} particles is clearly limited by the rate of DNA target permeation through the PEM film. Permeation of the different DNA targets through the PSS/(PAH/PSS)₃ shell is still observed after 72 h (Figure 7b). However, throughout the incubation period, the trend with respect to the relative permeation of the different DNA targets is unchanged (e.g., the 20 b target remains the most efficient) (Figure 7b). This suggests that the structure of the PSS/(PAH/PSS)₃ shell, and hence its permeability properties, do not change throughout the incubation period.

Table 2 compares the findings of this work with those of several earlier studies on the permeability of PSS/PAH multilayer capsules. The data suggest that magnesium/oxalate ions and ibuprofen diffuse through PSS/PAH multilayers at a similar rate, which is faster than that of fluorescein and significantly faster than that of the DNA targets used in this study. Although these rates are influenced by the conditions under which the capsules were prepared and probed, the relatively low diffusion coefficients obtained in this work are primarily ascribed to the DNA targets being significantly larger and less compact than the substances used in the earlier studies, and thus the DNA targets cannot permeate through the PSS/PAH multilayers as readily.

To our knowledge, there have been no detailed investigations into the diffusion of DNA through PEM films thus far. The migration of DNA in buffers/gels has, however, been studied by several research groups. For example, Nkodo et al.¹² have reported

(12) Nkodo, A. E.; Garnier, J. M.; Tinland, B.; Ren, H.; Desruisseaux, C.; McCormick, L. C.; Drouin, G.; Slater, G. W. *Electrophoresis* **2001**, *22*, 2424–2432.

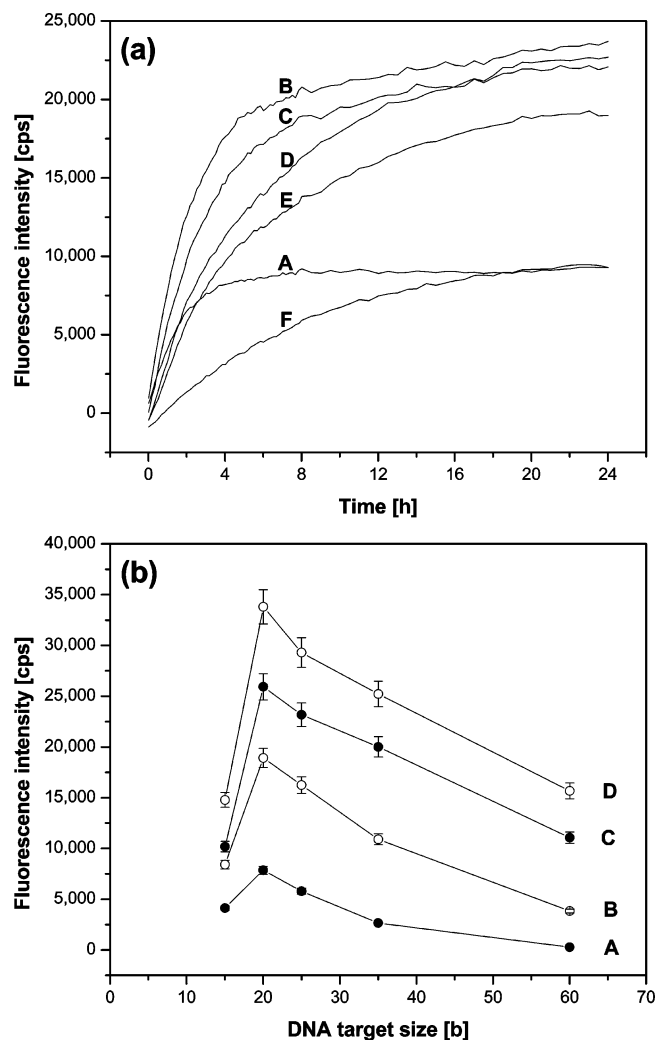


Figure 7. (a) Variation in MB fluorescence with time for BMS_{MB} particles encapsulated within PSS/(PAH/PSS)₃ after incubation with a (A) 15 b target, (B) 20 b target, (C) 25 b target, (D) 30 b target, (E) 35 b target, and (F) 60 b target. Assay conditions: BMS_{MB} particle concentration, 6×10^4 particles μL^{-1} ; MB/BMS ratio, 1:1; DNA target concentration, $3 \mu\text{M}$; pH, 7; NaCl concentration, 0.5 M. (b) Variation in MB fluorescence with DNA target size for BMS_{MB} particles encapsulated within PSS/(PAH/PSS)₃ after incubation for (A) 1 h, (B) 5 h, (C) 36 h, and (D) 72 h. Assay conditions are the same as those given in part a.

Table 2. Comparison of Diffusion Coefficients Obtained in This Work with Those Reported in Earlier Studies on the Permeability of PSS/PAH Multilayer Capsules

permeant	MW [Da]	diffusion coefficient [$\text{m}^2 \text{s}^{-1}$]	ref
$\text{Mg}^{2+}/\text{C}_2\text{O}_4^{2-}$	24/88	10^{-13}	5e
ibuprofen	206	10^{-13}	5c
fluorescein	332	10^{-16}	5a
DNA	4,681–18,551	10^{-19} – 10^{-18}	this work

diffusion coefficients of $\sim 10^{-11}$ – $10^{-10} \text{ m}^2 \text{ s}^{-1}$ for ssDNA fragments (18–250 b) in TBE (a buffer solution that consists of a mixture of Tris base, boric acid, ethylenediaminetetraacetic

acid, and water). Brahmastra *et al.*¹³ have reported diffusion coefficients of $\sim 10^{-14}$ – $10^{-11} \text{ m}^2 \text{ s}^{-1}$ for ssDNA fragments (50–500 b) in a polyacrylamide gel (a matrix of acrylamide polymers cross-linked using bisacrylamide). These values are several orders of magnitude greater than the diffusion coefficients reported here, indicating that the PEM films present a substantial resistance to the diffusion path of the DNA targets. Diffusion coefficients of a similar magnitude to those obtained in this work have been reported by Antonietti and Sillescu for the diffusion of branched polystyrene (PS) molecules (160 kDa) in PS microgel matrices¹⁴ and by Best and Sillescu for interdiffusion in blends of PS (16–35 kDa) and polymethylstyrene (40–407 kDa).¹⁵

Conclusions

The fundamental conditions underlying the MB–DNA sensing process (BMS_{MB} particle concentration, MB loading within the BMS particles, DNA target concentration, DNA target size, pH, NaCl concentration) were established. MB fluorescence was found to increase with the BMS_{MB} particle concentration, the MB loading within the BMS particles, the DNA target concentration, and the DNA target size. We also found that while acidic pH has a reversible effect on the MB–DNA sensing process, alkaline pH and high ionic strength have an irreversible effect.

BMS_{MB} particles encapsulated within PSS/(PAH/PSS)_x and PEI/PSS/(PAH/PSS)_x, where $x = 1, 2, 3, 4,$ or 6 , were used to probe the permeability of the PEM films via the MB approach. We observed that the permeability of the DNA targets decreases significantly with layer number ($2.1 \times 10^{-10} \text{ m s}^{-1}$ for 3 layers to $2.8 \times 10^{-11} \text{ m s}^{-1}$ for 7 layers) and that the presence of a PEI precursor layer promotes the growth of less permeable PSS/PAH multilayers. Furthermore, the studies on permeability as a function of DNA target size show that PSS/PAH capsules can be readily tuned through layer number to preferentially include/exclude certain DNA sequences and that the permeability properties of the capsules remain unchanged over periods of up to 72 h.

Future work will focus on using the MB approach to probe the permeability of different types of LbL capsules as a function of various parameters used to assemble the capsules. Different targets, for example, DNA–nanoparticle and DNA–protein conjugates, will also be examined.

Acknowledgment. We gratefully acknowledge the Australian Research Council for financial support (Discovery Project and Federation Fellowship schemes) and the Particulate Fluids Processing Centre for infrastructure support. We also thank Alexander Zelikin for providing the FITC-PSS and Anthony Quinn for his assistance with the fluorescence spectrophotometer.

Supporting Information Available: Plots of the variation in MB fluorescence with (i) BMS_{MB} particle concentration and (ii) time, for BMS_{MB} particles encapsulated within PSS/(PAH/PSS)₃. This material is available free of charge via the Internet at <http://pubs.acs.org>.

LA063674H

(13) Brahmastra, S. N.; Burke, D. T.; Mastrangelo, C. H.; Burns, M. A. *Electrophoresis* **2001**, *22*, 1046–1062.

(14) Antonietti, M.; Sillescu, H. *Macromolecules* **1986**, *19*, 798–803.

(15) Best, M.; Sillescu, H. *Polymer* **1992**, *33*, 5249–5253.